applied sciences

MDPI

Article

Biomechanical Evaluation of the Effect of Mesenchymal Stem Cells on Cartilage Regeneration in Knee Joint Osteoarthritis

Yong-Gon Koh [1], Jin-Ah Lee [2], Hwa-Yong Lee [2], Hyo-Jeong Kim [3] and Kyoung-Tak Kang [2,*]

[1] Joint Reconstruction Center, Department of Orthopaedic Surgery, Yonsei Sarang Hospital, 10 Hyoryeong-ro, Seocho-gu, Seoul 06698, Korea; osygkoh@gmail.com

[2] Department of Mechanical Engineering, Yonsei University, 50 Yonsei-ro, Seodaemun-gu, Seoul 03722, Korea; gna0812@gmail.com (J.-A.L.); au0707@gmail.com (H.-Y.L.)

[3] Department of Sport and Healthy Aging, Korea National Sport University, 1239 Yangjae-dearo, Songpa-gu, Seoul 05541, Korea; knsu.hjkim@gmail.com

* Correspondence: tagi1024@gmail.com; Tel.: +82-2-2123-4827; Fax: +82-2-362-2736

Received: 28 March 2019; Accepted: 25 April 2019; Published: 7 May 2019

Abstract: Numerous clinical studies have reported cell-based treatments for cartilage regeneration in knee joint osteoarthritis using mesenchymal stem cells (MSCs). However, the post-surgery rehabilitation and weight-bearing times remain unclear. Phenomenological computational models of cartilage regeneration have been only partially successful in predicting experimental results and this may be due to simplistic modeling assumptions and loading conditions of cellular activity. In the present study, we developed a knee joint model of cell and tissue differentiation based on a more mechanistic approach, which was applied to cartilage regeneration in osteoarthritis. First, a phenomenological biphasic poroelastic finite element model was developed and validated according to a previous study. Second, this method was applied to a real knee joint model with a cartilage defect created to simulate the tissue regeneration process. The knee joint model was able to accurately predict several aspects of cartilage regeneration, such as the cell and tissue distributions in the cartilage defect. Additionally, our results indicated that gait cycle loading with flexion was helpful for cartilage regeneration compared to the use of simple weight-bearing loading.

Keywords: stem cell; cartilage; finite element

1. Introduction

Osteoarthritis (OA) of the knee is the most common result of arthritis that leads to pain, stiffness and decreased mobility, with this disease being one of the major causes of disability among non-institutionalized adults [1,2]. OA is a process of cartilage degeneration that involves the immune system, in which local inflammatory responses are observed with the production of proinflammatory cytokines [3,4]. The articular cartilage possesses limited reparative abilities and the associated osteochondral defects present in young patients generally do not heal but usually progress to degeneration of the surrounding cartilage [5]. There are a limited number of treatment options available to improve or reverse the process [3,4]. Additionally, with the exception of joint replacement, the most common treatments for OA are not widely applied and can be associated with substantial adverse events, high costs or both [6].

Mesenchymal stem cells (MSCs) have been proposed to possess potential in the cell-based treatment of cartilage lesions [7]. These cells show great promise as a therapeutic agent in regenerative medicine due to their multilineage potential, immunosuppressive activities, limited immunogenicity and relative ease of growth in culture [7]. Additionally, MSCs represent an autologous cell source that

reduces the chance for rejection and disease transmission they are also less tumorigenic than their embryonic counterparts [8]. However, there are no studies that have quantitatively evaluated the degree of rehabilitation of an OA knee joint after injection or transplantation of MSCs.

Mechano-regulation algorithms have been suggested to evaluate the possible relationship between mechanical stimulation and the differentiation of cells and tissues [9–15]. These phenomenological computational models, however, have several problems, particularly regarding the general simplification, such as loading condition and simplified geometry [9–12]. Recently we studied to predict the mechanical properties of an optimum scaffold required for cartilage regeneration using three-dimensional knee joint developed from medical imaging and mechano-regulation theory [16].

Therefor, the aim of the present study was to investigate cartilage regeneration in OA or cartilage defects based on the knee joint mechano-regulation of MSC differentiation theory using a realistic model based on three-dimensional (3D) medical imaging. This model considers the effect of mechanical stimuli on cell mitosis and death and it also incorporates the influence of the tissues on cell dispersal rate We hypothesized that the prediction of mechano-regulated tissue differentiation would differ with respect to the loading conditions.

2. Materials and Methods

To investigate individual cellular model parameters of cartilage regeneration, a mechano-biological tissue-differentiation model that included theoretical descriptions of cellular processes was used according to a previous validation method [17]. This model has been employed to simulate the major aspects of normal conditions and cartilage regeneration [17,18]. Mechano-regulation processes are driven by the mechanical environment in the vicinity of the cell. A computational approach, such as finite element (FE) modeling, enables the evaluation of the mechanical stimuli within the extracellular matrix of a regenerating tissue. In this study, a cartilage defect within the knee joint was investigated using a poroelastic FE model. Briefly, the entire callus was assumed to consist of granulation tissue at the beginning of the stimulation regimen. Generally, once the subchondral bone is penetrated, MSCs invade the defect in the bone marrow. Given this, the stem cells were assumed to originate from the periosteum, outer cortical surface and medullary canal in a previous study [18]. This method was applied to generate the first phenomenological model. In the second model, adipose synovium-derived MSCs were used for cartilage defect implantation because we have had successful clinical experience with this approach [19–21].

To simulate the diffusion of stem cells throughout the callus, a diffusion coefficient was selected to predict 99% stem cell coverage at six weeks after implantation [12]. After this, the differentiation of the granulation tissue in a given element towards the fibrous tissue, cartilage or bone was determined by the stimulus factor (S) according to Equation (1):

$$S = \frac{\gamma}{a} + \frac{v}{b} \tag{1}$$

where γ is the octahedral shear strain, ν is the fluid velocity and a (3.75%) and b (3 μm/s) are the scaling factors for each stimulus. Based on the mechano-regulation theory, $S > 3$ is predicted as fibrous connective tissue, $1 < S < 3$ indicates cartilage, $0.53 < S < 1$ indicates immature woven bone, $0.01 < S < 0.53$ indicates mature woven bone and $0 < S < 0.01$ indicates bone resorption [4,12,13,18,19,22].

Poroelastic material properties were updated according to a rule of mixtures based on the concentration of cells in a given element (n_c), the volume fractions (φ_j) and material properties of the granulation tissue and j types of differentiated tissues in that element. For example, Young's modulus (E) for a given element was calculated according to Equation (2):

$$\mathrm{E} = \frac{(n_c^{max} - n_c)}{n_c^{max}} E_{granulation} + \frac{n_c}{n_c^{max}} \sum_{j=1}^{n_t} E_j \varphi_j \tag{2}$$

where n_c^{max} is the maximum number of cells that can occupy any single element and Ej is Young's Modulus of the jth differentiated tissue. The volume fraction φ_j of a given type of differentiated tissue was evaluated as the fraction of the last ten iterations for which this particular differentiated tissue type was predicted in the element. This enabled the material properties to change gradually and prevented instability in the algorithm [23]. Material property was calculated for each element by this formula using a custom FORTRAN script.

The two poroelastic FE models were developed to simulate in vivo mechnical conditions within knee joint OA mechano-regulation under different loading conditions. The first phenomenological axi-symmetric FE model of the knee was created, which included a meniscus, femoral condyle and articular cartilage layer to validate this approach (Figure 1). The pore fluid pressure was adjusted to zero at free. The meniscus and the cartilage surface could not penetrate each other in the axial direction. However, the surfaces were allowed to slide relative to each other. The cartilage defect size and depth were set at 5 mm each. Complete integration was assumed between the repair tissue and normal tissue. An axial ramp load of 800 N was applied for 0.5 s. All tissues were modeled as being biphasic based on the poroelastic theory. The material properties used for each tissue type are shown in Table 1. The meniscus was modeled as transversely isotropic and poroelastic with a higher stiffness in the circumferential direction [12].

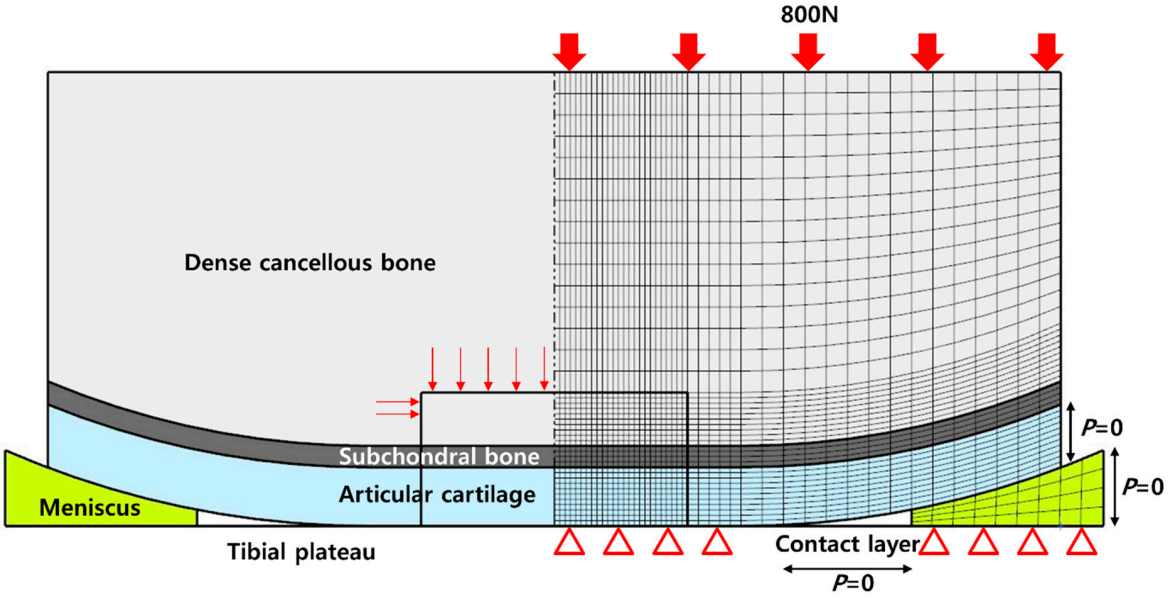

Figure 1. Schematic of the phenomenological axi-symmetric FE model of the knee including a femoral condyle, articular cartilage layer and meniscus for validation.

Table 1. Material properties used in this simulation.

	Granulation Tissue	Fibrous Tissue	Cartilage	Immature Bone	Mature Bone	Cortical Bone
Young's modulus (MPa)	0.2	2	10	1000	6000	17,000
Poisson's ratio (ν)	0.167	0.167	0.167	0.3	0.3	0.3
Permeability $\left(m^4/N_s \times 10^{-14}\right)$	1	1	0.5	0.1	0.37	0.001
Porosity	0.8	0.8	0.8	0.8	0.8	0.04
Diffusion coefficient (mm^2/iteration)	0.8	0.1	0.05	0.01	0.01	-

The second poroelastic FE model of the knee joint (Figure 2c) was developed from real medical imaging based on a previously reported model [24–26] that was further developed. Briefly, a 3D FE model of a normal knee joint was developed using data from computed tomography (CT) (Figure 2a) and magnetic resonance imaging (MRI) scans (Figure 2b) of a healthy 37-year-old male subject. The CT and MRI models were developed with a slice thickness of 0.1 mm and 0.4 mm, respectively. Unlike the phenomenological model, this model was developed specifically for the tibial cartilage to describe an actual clinical situation. Contact was modeled between the femoral cartilage and the meniscus, the meniscus and the tibial cartilage and the femoral cartilage and the tibial cartilage for both the medial and lateral sides, which resulted in a total of six contact pairs. In short, the components were not penetrating. The second model developed at 64 mm^2 with a depth of 3 mm. Two loading conditions were applied. The first condition was an axial ramp load of 1750 N, which was the same as that applied in the phenomenological model, and the second was a stance-phase gait cycle derived from the ISO14,243-1 standard [27]. All FE analyses were completed using ABAQUS 6.5 (Abaqus, Inc., East Providence, RI, USA) and the mechano-regulation theory was a user-defined subroutine constructed by the FORTRAN code.

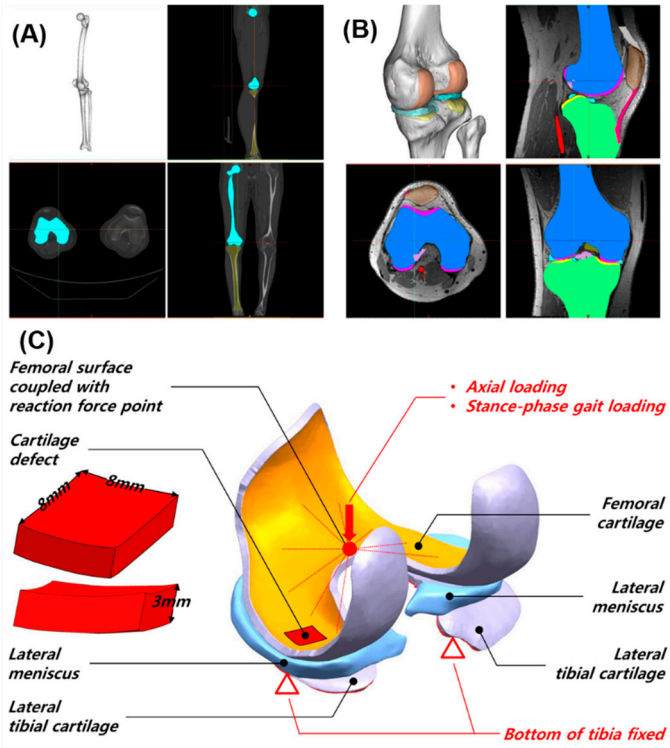

Figure 2. A realistic 3D knee joint model developed using data from (**a**) CT and (**b**) MRI scans. (**c**) Schematic representations of the cartilage defect model and the boundary conditions for cartilage regeneration prediction.

3. Results

Figure 3 presents the phenomenological computational model of predicted patterns of tissue differentiation in cartilage defects. This results in higher cell death predictions in the superficial layer of the repair tissue as MSCs differentiate into fibroblasts and undergo death in the high-strain environment. This trend was also observed in a previous study [9].

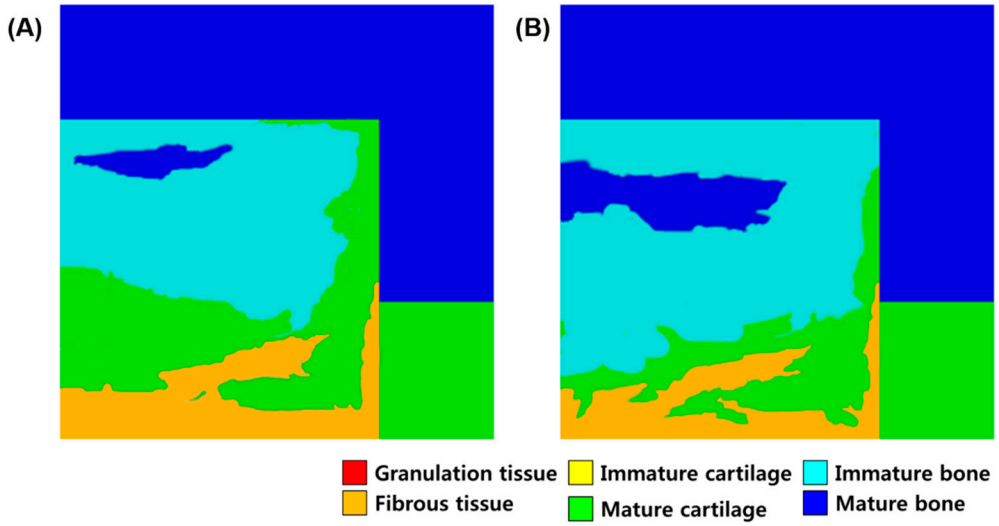

Figure 3. Predicted patterns of tissue differentiation with 5 mm cartilage defect in a simulation of (**a**) 25 iterations and (**b**) 50 iterations.

The cell concentration and each tissue type formation observed in this study and Kelly and Prendergast's study were compared in Figure 4 [9]. A minor difference was observed, but the overall trend is consistent. In particular, there were similar predictions for the simulated fibrous tissue formation (18% in the present study and 16% in the previous study) and bone formation (61% in the present study and 64% in the previous study) [9].

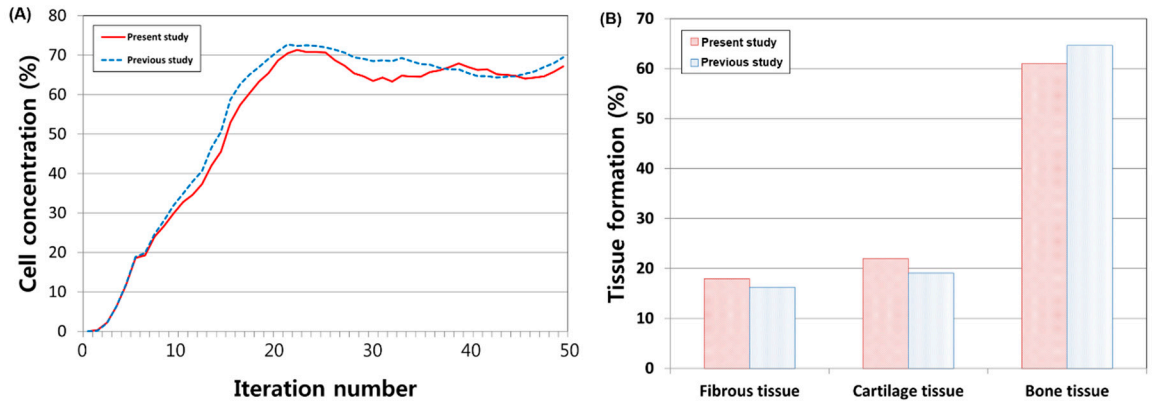

Figure 4. Comparison of prediction of (**a**) cell concentration at the articular surface and (**b**) percentage of tissue types between this study and a previous study [9] for validation.

Figure 5 shows the pattern of regeneration of the cartilage defect in the knee joint model for axial and stance-phase gait cycle loadings. The predicted patterns of tissue differentiation after MSC implantation in the stance-phase gait cycle condition model were found to be remarkably different from those predicted by the axial force model. The stance-phase gait model was predicted to support early chondrogenesis, with the chondral region of the defect consisting primarily of immature cartilage tissue. Increased cartilage formation was predicted as the simulation of the defect repair progressed and a remarkably greater proportion of the defect consisted of cartilage tissue. A strong uniform band of fibrous tissue was maintained at the articular cartilage. Additionally, the remainder of the chondral portion of the defect consisted of cartilage tissue. However, in the axial force model, the simulations showed that the defect was partially shielded by the adjacent intact cartilage and the stimulus within the defect was low. As the regenerated tissue begins to stiffen, it begins to support loads and chondrogenesis is favored within the center of the defect. After a given period of time,

increased bone formation is predicted to occur by endochondral ossification and particular regions of cartilage begin to differentiate into fibrous tissue, ultimately resulting in a reduction in the amount of cartilage within the defect. Figure 6 showed cell concentration in axial force model and stance phase gait model. Axial force model cell death was found in articular surface, but stance phase gait model cell death was prevented because rotation or translation because controlled axial force was exerted only at the defect region. Figure 7 shows tissue type formation after 40 iterations in axial force model in stance phase gait model. In 40 iterations, greater amounts of cartilage tissue formation were predicted, with 56% in the stance-phase gait model and 29% in the axial force model.

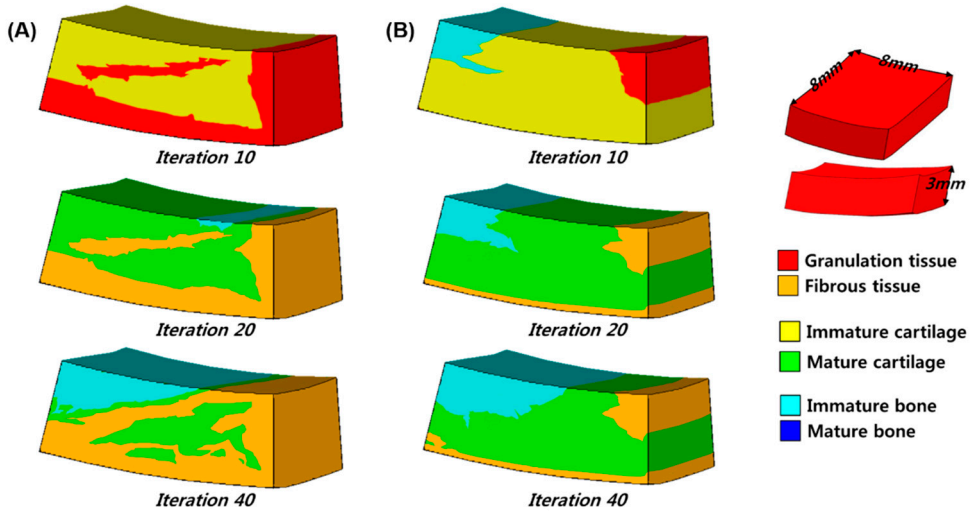

Figure 5. Pattern of regeneration of the cartilage defect in the knee joint model in 10, 20 and 40 iterations for (**a**) axial and (**b**) stance-phase gait cycle loading.

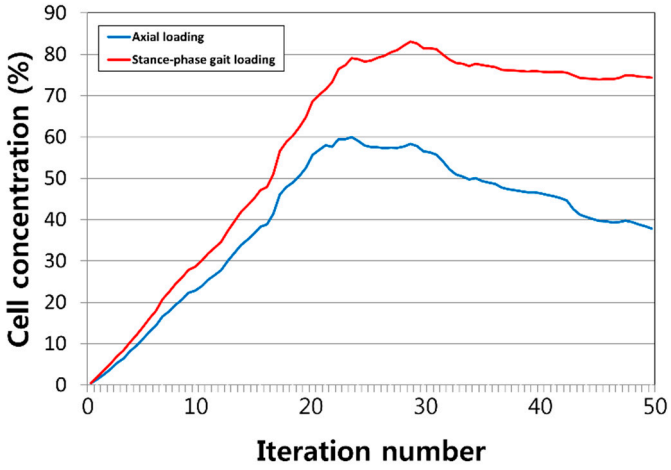

Figure 6. Comparison of the prediction of cell concentration between the axial loading and the stance-phase gait loading model.

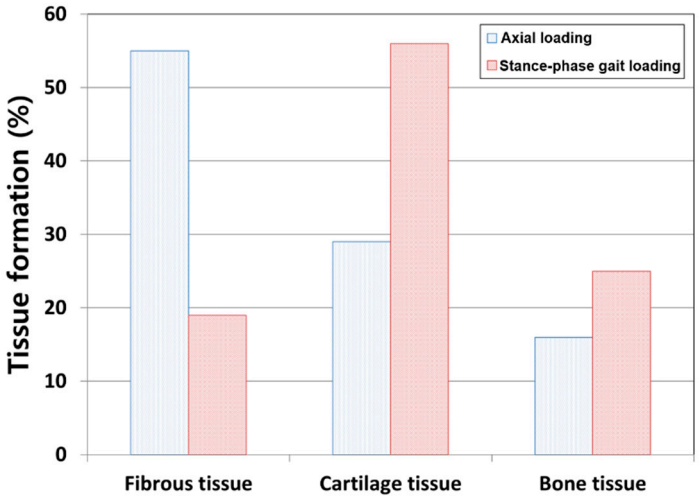

Figure 7. Percentage of each tissue type formation in the axial loading and the stance-phase gait loading model after 40 iterations.

4. Discussion

The most important finding of this study was that different results were found with respect to the loading conditions in a real knee joint model for mechano-biological tissue differentiation.

Cartilage defects possess a very limited intrinsic healing capacity. Curl et al. described 53,569 hyaline cartilage lesions in 19,827 patients that received total knee arthroplasty [28]. Similarly, a more recent prospective survey of 993 consecutive knee arthroscopies showed evidence of articular cartilage abnormality in 66% of the patients [29]. Several techniques for articular cartilage defect treatment have been described recently with various results and indications [24,30]. Microfracture represents a widely used technique for the repair of symptomatic articular cartilage defects of the knee [31,32]. The penetration of the subchondral bone plate in these defects causes clot formation in the defect. This clot contains pluripotent, marrow-derived MSCs, which can induce fibrocartilage repair as they possess varying amounts of type II collagen [30]. However, the microfracture technique is limited for treating large-sized defects. Small defects can spontaneously undergo repair with the hyaline cartilage, while larger defects undergo repair only with fibrous tissue or fibrocartilage, which are biochemically and biomechanically different from normal hyaline cartilage [3]. A recent review paper indicated that osteochondral autograft transfer may achieve higher activity levels and a lower risk of failure compared to the microfracture technique for cartilage lesions greater than 3 cm^2, although there was no significant difference for lesions smaller than 3 cm^2 at midterm [33]. Therefore, degeneration may occur, which can subsequently progress to osteoarthritic changes [34].

Recently, MSCs have been recommended for use in the cell-based treatment of cartilage lesions. Chondrogenesis of MSCs was primarily reported by Ashton et al. [35] and a defined medium for the in-vitro chondrogenesis of MSCs was primarily reported by Johnstone et al. [36], who used micromass culture with transforming growth factor-beta and dexamethasone. With regard to the in-vivo studies, the transplantation of MSCs into full-thickness articular cartilage defects has been attempted under various conditions. Some studies recently reported that adipose-derived MSCs therapy for young and even elderly patients with knee OA was effective with respect to cartilage healing, reducing pain and improving function [19–21]. Additionally, Kim et al. demonstrated that the implantation of MSCs for knee OA resulted in improved clinical and second-look arthroscopic outcomes compared to those reported after an injection of MSCs [37]. Another recent study recommended that non-weight-bearing conditions with only toe-touching for 8 weeks may have similar effects to those achieved within the period used in other treatments for cartilage regeneration when MSCs were injected to OA patients [38]. However, the authors also stated that although this prolonged period of non-weight-bearing may enable some native repair, it decreased and delayed the recovery of knee function after injections

as evidenced by an initial decline of the Knee Society Clinical Rating System function score [38]. Therefore, an optimal rehabilitation protocol for the injection and implantation of MSCs should be further investigated and determined.

To date, the Prendergast mechano-regulation theory has been applied to a number of different scenarios of bone healing and cartilage regeneration and it has displayed tremendous promise as a theory that could accurately describe the course of mesenchymal tissue differentiation in response to a wide spectrum of mechanical conditions [12,17,18]. However, all of these studies performed simulations from a microfracture perspective [12,17,18,39]. Moreover, the stem cells were assumed to originate from the periosteum, the outer cortical surface and medullary canal according to mechano-regulation tissue differentiation [12,17,18,39].

The objective of the present study was to perform a robust test of this theory by applying it to a MSC implantation model in knee OA where different mechanical loadings were used to alter the cartilage regeneration response. One of the main strengths of this study is that the modeling technique used to test the mechano-regulation theory is dissimilar to those typically used to investigate the mechano-regulation of cartilage regeneration. Many previous computational studies examining the mechano-biology of cartilage regeneration only investigated the physiological axial load. Additionally, they described boundary and contact conditions that do not accurately reflect clinical situations using simple phenomenological computational models. Our knee joint model that was developed from real medical imaging could successfully predict the patterns of cellular differentiation in osteochondral defect regeneration. A previous study demonstrated regeneration through both endochondral and direct intramembranous ossification in the base of the defect, with cartilage formation occurring at the center of the defect and fibrous tissue formation superficially [40]. This pattern of repair was also found in the present model. We also found that gait cycle loading was better than vertical loading for cartilage regeneration. However, in the simple vertical loading model, increased bone formation was predicted to occur via endochondral ossification and particular regions of the cartilage began to differentiate into fibrous tissue, ultimately leading to a reduction in the amount of cartilage within the defect. Due to an increase in the magnitude of fluid flow within the defect, the stimulus for fibrous tissue formation is increased [41]. This increase in strain also promotes cell death at the articular surface [41]. Thus, preventing this fibrous tissue formation superficially and any subsequent cell death by an appropriate rehabilitation protocol would be beneficial in avoiding long-term failure of tissue repair.

There are also several limitations to this study. First, we assumed that cell movement can be described using a diffusion equation of a non-linear relationship that exists between mitosis/cell death and the magnitude of strain experienced by cells; and that tissue differentiation is regulated by a combination of the magnitude of octahedral shear strain and fluid flow within the tissue, which may not be completely accurate. Second, we did not account for the rate at which cells differentiate and produce a matrix and we did not attempt to model the effects of growth factors, such as transforming growth factor-beta. Third, we did not model the scaffold. The MSCs are not actually injected directly but should rather be implanted in combination with a scaffold.

Fourth, our model could not be validated using experimental data. It is very challenging to find experimental data with identical conditions. There are also advantages of using computational simulations to predict the results in this way. In addition, we validated it with previous computational results.

Finally, the developed models did not consider cells that only migrate into the defect from the exposed cancellous bone and it was instead assumed that MSCs could only enter the defect through implantation.

Developments of computational technology have now enabled researchers to perform simulations from a patient- or subject-specific perspective in the orthopedic field. Our results were obtained using a 3D model developed from real medical imaging and our results demonstrate that stance-phase loading was better than axial loading for cartilage regeneration. This is because simple vertical loading may cause excessive strain, while a stance-phase gait cycle prevents this strain at the cartilage defect due

to the relationship with other loadings. The advantage of using such an approach is that it is one of the key features of computational methods in tissue engineering that enables the expedition of the testing of new constructs and the development of strategies for identifying the optimal therapy for each patient [42]. From this perspective, our results could provide patient-specific rehabilitation guidelines for the implantation of MSCs.

In conclusion, we developed a computational approach to simulate tissue differentiation that was tested by attempting to simulate cartilage regeneration and the results yielded tissue formation patterns similar to those observed clinically. Although we found that a stance-phase gait was better than axial loading in the context of cartilage regeneration, a more complex study protocol is required for future investigations and such a protocol should include consideration of the effects of passive flexion after axial force or crutches in weight-bearing.

Author Contributions: Y.G.K. designed the study, evaluated the FEA results and wrote the paper; J.A.L. developed the 3D model; K.T.K. supervised the study and analyzed the data; H.Y.L. confirmed data; H.Y.K. review the paper.

Funding: This research received no external funding.

Acknowledgments: No external funding was received for the study.

Conflicts of Interest: The authors declare no conflicts of interest.

References

1. Lawrence, R.C.; Felson, D.T.; Helmick, C.G.; Arnold, L.M.; Choi, H.; Deyo, R.A.; Gabriel, S.; Hirsch, R.; Hochberg, M.C.; Hunder, G.G.; et al. Estimates of the prevalence of arthritis and other rheumatic conditions in the united states. Part ii. *Arthritis Rheum.* **2008**, *58*, 26–35. [CrossRef]
2. Dillon, C.F.; Rasch, E.K.; Gu, Q.; Hirsch, R. Prevalence of knee osteoarthritis in the united states: Arthritis data from the third national health and nutrition examination survey 1991–94. *J. Rheumatol.* **2006**, *33*, 2271–2279.
3. Koh, Y.G.; Choi, Y.J. Infrapatellar fat pad-derived mesenchymal stem cell therapy for knee osteoarthritis. *Knee* **2012**, *19*, 902–907. [CrossRef] [PubMed]
4. Mankin, H.J. The response of articular cartilage to mechanical injury. *J. Bone Jt. Surg.* **1982**, *64*, 460–466. [CrossRef]
5. Kim, H.K.; Moran, M.E.; Salter, R.B. The potential for regeneration of articular cartilage in defects created by chondral shaving and subchondral abrasion. An experimental investigation in rabbits. *J. Bone Jt. Surg. Am. Vol.* **1991**, *73*, 1301–1315. [CrossRef]
6. Lohmander, L.S.; Roos, E.M. Clinical update: Treating osteoarthritis. *Lancet (Lond. Engl.)* **2007**, *370*, 2082–2084. [CrossRef]
7. Beitzel, K.; McCarthy, M.B.; Cote, M.P.; Chowaniec, D.; Falcone, L.M.; Falcone, J.A.; Dugdale, E.M.; Deberardino, T.M.; Arciero, R.A.; Mazzocca, A.D. Rapid isolation of human stem cells (connective progenitor cells) from the distal femur during arthroscopic knee surgery. *Arthrosc. J. Arthrosc. Relat. Surg. Off. Publ. Arthrosc. Assoc. N. Am. Int. Arthrosc. Assoc.* **2012**, *28*, 74–84. [CrossRef]
8. Raghunath, J.; Salacinski, H.J.; Sales, K.M.; Butler, P.E.; Seifalian, A.M. Advancing cartilage tissue engineering: The application of stem cell technology. *Curr. Opin. Biotechnol.* **2005**, *16*, 503–509. [CrossRef] [PubMed]
9. Kelly, D.J.; Prendergast, P.J. Mechano-regulation of stem cell differentiation and tissue regeneration in osteochondral defects. *J. Biomech.* **2005**, *38*, 1413–1422. [CrossRef] [PubMed]
10. Ament, C.; Hofer, E.P. A fuzzy logic model of fracture healing. *J. Biomech.* **2000**, *33*, 961–968. [CrossRef]
11. Prendergast, P.J.; Huiskes, R.; Søballe, K. Biophysical stimuli on cells during tissue differentiation at implant interfaces. *J. Biomech.* **1997**, *30*, 539–548. [CrossRef]
12. Isaksson, H.; van Donkelaar, C.C.; Huiskes, R.; Ito, K. A mechano-regulatory bone-healing model incorporating cell-phenotype specific activity. *J. Theor. Biol.* **2008**, *252*, 230–246. [CrossRef] [PubMed]
13. Nagel, T.; Kelly, D.J. Mechano-regulation of mesenchymal stem cell differentiation and collagen organisation during skeletal tissue repair. *Biomech. Model. Mechanobiol.* **2010**, *9*, 359–372. [CrossRef] [PubMed]
14. O'Reilly, A.; Kelly, D.J. Role of oxygen as a regulator of stem cell fate during the spontaneous repair of osteochondral defects. *J. Orthop. Res. Off. Publ. Orthop. Res. Soc.* **2016**, *34*, 1026–1036. [CrossRef] [PubMed]

15. O'Reilly, A.; Kelly, D.J. A computational model of osteochondral defect repair following implantation of stem cell-laden multiphase scaffolds. *Tissue Eng. Part A* **2017**, *23*, 30–42. [CrossRef]
16. Koh, Y.G.; Lee, J.A.; Kim, Y.S.; Lee, H.Y.; Kim, H.J.; Kang, K.T. Optimal mechanical properties of a scaffold for cartilage regeneration using finite element analysis. *J. Tissue Eng.* **2019**, *10*, 2041731419832133. [CrossRef] [PubMed]
17. Lacroix, D.; Prendergast, P.J.; Li, G.; Marsh, D. Biomechanical model to simulate tissue differentiation and bone regeneration: Application to fracture healing. *Med. Biol. Eng. Comput.* **2002**, *40*, 14–21. [CrossRef]
18. Hayward, L.N.; Morgan, E.F. Assessment of a mechano-regulation theory of skeletal tissue differentiation in an in vivo model of mechanically induced cartilage formation. *Biomech. Model. Mechanobiol.* **2009**, *8*, 447–455. [CrossRef] [PubMed]
19. Kim, Y.S.; Choi, Y.J.; Suh, D.S.; Heo, D.B.; Kim, Y.I.; Ryu, J.S.; Koh, Y.G. Mesenchymal stem cell implantation in osteoarthritic knees: Is fibrin glue effective as a scaffold? *Am. J. Sports Med.* **2015**, *43*, 176–185. [CrossRef] [PubMed]
20. Koh, Y.G.; Choi, Y.J.; Kwon, O.R.; Kim, Y.S. Second-look arthroscopic evaluation of cartilage lesions after mesenchymal stem cell implantation in osteoarthritic knees. *Am. J. Sports Med.* **2014**, *42*, 1628–1637. [CrossRef] [PubMed]
21. Kim, Y.S.; Choi, Y.J.; Koh, Y.G. Mesenchymal stem cell implantation in knee osteoarthritis: An assessment of the factors influencing clinical outcomes. *Am. J. Sports Med.* **2015**, *43*, 2293–2301. [CrossRef] [PubMed]
22. Isaksson, H.; Van Donkelaar, C.C.; Huiskes, R.; Yao, J.; Ita, K. Determining the most important cellular characteristics for fracture healing using design of experiments methods. *J. Theor. Biol.* **2008**, *255*, 26–39. [CrossRef]
23. Lacroix, D.; Prendergast, P.J. A homogenization procedure to prevent numerical instabilities in poroelastic tissue differentiation models. In Proceedings of the Eighth Annual Symposium: Computational Methods in Orthopaedic Biomechanics, Lake Buena Vista, FL, USA, 11 March 2000.
24. Kang, K.T.; Kim, S.H.; Son, J.; Lee, Y.H.; Chun, H.J. Computational model-based probabilistic analysis of in vivo material properties for ligament stiffness using the laxity test and computed tomography. *J. Mater. Sci. Mater. Med.* **2016**, *27*, 183. [CrossRef]
25. Koh, Y.G.; Son, J.; Kwon, S.K.; Kim, H.J.; Kwon, O.R.; Kang, K.T. Preservation of kinematics with posterior cruciate-, bicruciate- and patient-specific bicruciate-retaining prostheses in total knee arthroplasty by using computational simulation with normal knee model. *Bone Jt. Res.* **2017**, *6*, 557–565. [CrossRef] [PubMed]
26. Kang, K.T.; Koh, Y.G.; Son, J.; Kim, S.J.; Choi, S.; Jung, M.; Kim, S.H. Finite element analysis of the biomechanical effects of 3 posterolateral corner reconstruction techniques for the knee joint. *J. Arthrosc.* **2017**, *33*, 1537–1550. [CrossRef]
27. 14243-1, I. Implants for surgery—wear of total knee-joint prostheses—part 1: Loading and displacement parameters for wear-testing machines with load control and corresponding environmental conditions for test. 2009.
28. Curl, W.W.; Krome, J.; Gordon, E.S.; Rushing, J.; Smith, B.P.; Poehling, G.G. Cartilage injuries: A review of 31,516 knee arthroscopies. *Arthrosc. J. Arthrosc. Relat. Surg. Off. Publ. Arthrosc. Assoc. N. Am. Int. Arthrosc. Assoc.* **1997**, *13*, 456–460. [CrossRef]
29. Aroen, A.; Loken, S.; Heir, S.; Alvik, E.; Ekeland, A.; Granlund, O.G.; Engebretsen, L. Articular cartilage lesions in 993 consecutive knee arthroscopies. *Am. J. Sports Med.* **2004**, *32*, 211–215. [CrossRef]
30. Mithoefer, K.; Williams, R.J., 3rd; Warren, R.F.; Potter, H.G.; Spock, C.R.; Jones, E.C.; Wickiewicz, T.L.; Marx, R.G. The microfracture technique for the treatment of articular cartilage lesions in the knee. A prospective cohort study. *J. Bone Jt. Surg. Am. Vol.* **2005**, *87*, 1911–1920. [CrossRef]
31. Steadman, J.R.; Briggs, K.K.; Rodrigo, J.J.; Kocher, M.S.; Gill, T.J.; Rodkey, W.G. Outcomes of microfracture for traumatic chondral defects of the knee: Average 11-year follow-up. *Arthrosc. J. Arthrosc. Relat. Surg. Off. Publ. Arthrosc. Assoc. N. Am. Int. Arthrosc. Assoc.* **2003**, *19*, 477–484. [CrossRef] [PubMed]
32. Steadman, J.R.; Rodkey, W.G.; Rodrigo, J.J. Microfracture: Surgical technique and rehabilitation to treat chondral defects. *Clin. Orthop. Relat. Res.* **2001**, *S391*, S362–S369. [CrossRef]
33. Pareek, A.; Reardon, P.J.; Macalena, J.A.; Levy, B.A.; Stuart, M.J.; Williams, R.J., 3rd; Krych, A.J. Osteochondral autograft transfer versus microfracture in the knee: A meta-analysis of prospective comparative studies at midterm. *Arthrosc. J. Arthrosc. Relat. Surg. Off. Publ. Arthrosc. Assoc. N. Am. Int. Arthrosc. Assoc.* **2016**, *32*, 2118–2130. [CrossRef]

34. Shelbourne, K.D.; Jari, S.; Gray, T. Outcome of untreated traumatic articular cartilage defects of the knee: A natural history study. *J. Bone Jt. Surg. Am. Vol.* **2003**, *85A* (Suppl. 2), 8–16. [CrossRef]
35. Ashton, B.A.; Allen, T.D.; Howlett, C.R.; Eaglesom, C.C.; Hattori, A.; Owen, M. Formation of bone and cartilage by marrow stromal cells in diffusion chambers in vivo. *Clin. Orthop. Relat. Res.* **1980**, *151*, 294–307. [CrossRef]
36. Johnstone, B.; Hering, T.M.; Caplan, A.I.; Goldberg, V.M.; Yoo, J.U. In vivo chondrogenesis of bone marrow-derived mesenchymal progenitor cells. *Exp. Cell Res.* **1998**, *238*, 265–272. [CrossRef] [PubMed]
37. Kim, Y.S.; Kwon, O.R.; Choi, Y.J.; Suh, D.S.; Heo, D.B.; Koh, Y.G. Comparative matched-pair analysis of the injection versus implantation of mesenchymal stem cells for knee osteoarthritis. *Am. J. Sports Med.* **2015**, *43*, 2738–2746. [CrossRef] [PubMed]
38. Jo, C.H.; Lee, Y.G.; Shin, W.H.; Kim, H.; Chai, J.W.; Jeong, E.C.; Kim, J.E.; Shim, H.; Shin, J.S.; Shin, I.S.; et al. Intra-articular injection of mesenchymal stem cells for the treatment of osteoarthritis of the knee: A proof-of-concept clinical trial. *Stem Cells (Dayt. Ohio)* **2014**, *32*, 1254–1266. [CrossRef] [PubMed]
39. Lacroix, D.; Prendergast, P.J. A mechano-regulation model for tissue differentiation during fracture healing: Analysis of gap size and loading. *J. Biomech.* **2002**, *35*, 1163–1171. [CrossRef]
40. Shapiro, F.; Koide, S.; Glimcher, M.J. Cell origin and differentiation in the repair of full-thickness defects of articular cartilage. *J. Bone Jt. Surg. Am. Vol.* **1993**, *75*, 532–553. [CrossRef]
41. Kelly, D.J.; Prendergast, P.J. Prediction of the optimal mechanical properties for a scaffold used in osteochondral defect repair. *Tissue Eng.* **2006**, *12*, 2509–2519. [CrossRef] [PubMed]
42. Semple, J.L.; Woolridge, N.; Lumsden, C.J. In vitro, in vivo, in silico: Computational systems in tissue engineering and regenerative medicine. *Tissue Eng.* **2005**, *11*, 341–356. [CrossRef] [PubMed]